

Fusion Reactions Involving Radioactive Beams at GANIL

Gilles DE FRANCE

GANIL, BP55027 F-14076 CAEN cedex 5, France

The ISOL type SPIRAL facility at GANIL has been commissioned recently and delivers radioactive beams (RIBs) for physics since a couple of years. Despite many difficulties arising from both the complexity to produce good beam quality and intensity as well as to setup the appropriate detection system, the first experiments with SPIRAL have demonstrated that nuclear dynamics studies (nuclear structure and low energy reaction mechanism) at the Coulomb barrier are possible with that kind of beams. RIBs like ^{76}Kr and $^{6,8}\text{He}$ have been used to produce exotic nuclei via fusion evaporation or to study reaction mechanisms at low energy. These two examples will be detailed in this talk.

§1. Introduction

The GANIL facility is based on the use of several cyclotrons running in cascade. For stable beam production and acceleration, two large separated sectors cyclotrons (CSS1 and CSS2) are used after the injector cyclotron. By using the successive output, it deliver beams from Carbon to Uranium in several energy windows:

- i*) at very low energy (0.3 to 1.0 MeV/A) directly from the injector cyclotron for solid state and atomic physics
- ii*) at medium energy (5.0 to 13.0 MeV/A) at the exit of a first large separated sector cyclotron (CSS1).
- iii*) at high energy (27.0 to 95.0 MeV/A) after the second cyclotron (CSS2). This is the usual regime for nuclear dynamics research looking for liquid-gaz phase transition (multifragmentation) for instance.

Apart from the production and use of these stable beams, GANIL is one of the laboratory where very exotic nuclei are extensively studied. To produce these rare, radioactive species, two distinct methods are used: the fragmentation technique and the Isotopic Separation On-Line (ISOL) method.

In the first case, the high energy beam from the second cyclotron is fragmented onto a target (the *production* target usually made of natural Nickel or Beryllium). The exotic nuclei issued from the fragmentation process are then selected according their magnetic rigidity ($B\rho$ proportional to the q/M ratio) by a standard spectrometer. A very special device, called SISSI, is used at GANIL in this context. It consists in two superconducting solenoids surrounding the production target. The aim of this technique is to very efficiently refocus the species after their production by the fragmentation mechanism, and to optimise the transmission into the spectrometer. In many examples, this method enhance the final global transmitted rates. However, it is not always the case since the acceptance (in terms of magnetic rigidity) is sometime the limiting factor for this technique. Once the species of interest have been produced and selected, they are transmitted either directly to a usual spectrometer (to measure their masses for instance) or to an achromatic spectrometer for further

selection and “beam” purification. The remaining nuclei can then be implanted and their decay studied. In both cases, the selected radioactive nuclei can also be used as a projectile on a secondary target. Since the beam intensity is seriously reduced as compared to the primary stable beam (several orders of magnitude), the cross section for the secondary reaction mechanism has to be rather large. Coulomb excitation is a typical example used to study the structure of the exotic projectile. Other reaction mechanisms like transfer or a secondary fragmentation are also used to produce even more exotic isotopes. The production of rare isotopes by the fragmentation technique is a powerful method but one intrinsic limitation resides in the rather thin production target (mandatory to avoid too much energy straggling and therefore limited transmission).

The second technique, the ISOL one, uses instead a very thick target. This is what is done at the SPIRAL facility at GANIL. The intense and high energy primary beam from the second cyclotron is sent on a very thick Carbone targets where it is again fragmented. The structure of the targets as well as the working temperature (~ 2300 °C) is made in such a way that the diffusion-effusion process of the exotic nuclei produced by fragmentation out of the Carbone is maximized. All the species are then collected into a permanent magnet ECRIS source and ionized. After extraction, the low energy RIB are selected in a separator and injected into the new $K = 265$ CIME cyclotron. Finally, after acceleration in the 1.7 MeV/A to 25.0 MeV/A energy range, the radioactive beams are sent into the GANIL existing experimental areas.

The SPIRAL facility,¹⁾ has started to deliver beams for experiments in fall 2001. The very first beam produced and accelerated with CIME was ^{18}Ne produced by a primary beam of $^{20}\text{Ne}^{10+}$ at an energy of 95 MeV/A. With a primary beam intensity of 1.6 mA (300 W), the ^{18}Ne secondary beam at 7.2 MeV/A has been measured to be 10^6 pps as expected. Later on, several campaigns of experiments have taken place using essentially ^{18}Ne , $^6,^8\text{He}$ and $^{74,76}\text{Kr}$ beams.

To accompany the development of these beams, new detectors have been designed and built. This is true more specifically for EXOGAM, a gamma-ray spectrometer dedicated to the physics with SPIRAL beams (and more generally to gamma-ray spectroscopy at low and medium multiplicity, typically less than $M_\gamma \sim 15$) and VAMOS a large acceptance spectrometer. In the following I will discuss the first *fusion* experiments using EXOGAM and radioactive beam from SPIRAL. I will first start by giving some details on the EXOGAM array.

§2. The EXOGAM array

A detailed presentation of the EXOGAM array can be found in Ref. 2). In this talk only the main characteristics of the spectrometer will be given.

The EXOGAM array has been designed to optimally exploit the use of radioactive beams delivered by SPIRAL. This has imposed severe constraints on the design specifications: large efficiency for low and medium gamma-ray multiplicity; good signal-to-noise ratio; coupling with many auxiliary devices to cope with the various experimental conditions. These requirements end up with a design using 16 Comp-

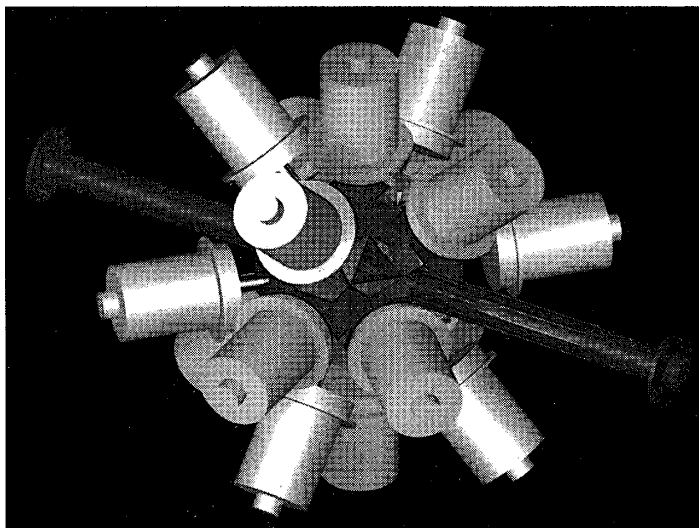


Fig. 1. Scheme of the EXOGAM array in its 16 Clover configuration. The anti-Compton shields are not represented.

ton suppressed large Clovers giving a photopeak efficiency of about 20% for a single gamma of $E_\gamma = 1.3$ MeV. The array (Fig. 1) has a versatile geometry which allows us to have various configurations: a compact configuration (conf. A) where the detectors are located at about 11 cm from the target and a pulled-back configuration (conf. B) where the distance is 15 cm.

The four Ge crystals composing the Clover are 9 cm long and have a diameter of 6 cm before shaping. They are tapered over 3 cm with an angle of 22.5 degrees. Each diode is electrically segmented in 4 in order to enhance the Doppler correction capability of the detectors.

The shield anti Compton design is based on 3 distinct layers and can be setup in two distinct configurations A and B. The first layer is the back catcher in CsI; the second one, the side catcher, is made of BGO and surrounds the rear part of the clover while the tapered length of the Ge cans is not covered; the third layer, the side shield, is a long piece in BGO which covers the whole Clovers starting from 2 cm before the Ge front face to the backcatcher. In conf. A, the shield consists of the two first layers: the back- and the side-catcher. The Ge are positionned in such a way that their tapered faces are in contact. This optimize the efficiency. In particular at very low gamma ray multiplicity, it is possible to add the energy deposited in neighbouring clovers without loosing too much with pile up effects (the *inter-Clover addback*). The gain in efficiency is about 10%. When the multiplicity is larger, leading in the close packed configuration to a very large amount of pile-up, the detectors are pulled back in configuration B and the additional side shield can be mounted to significantly enhance the peak-to-total ratio. The calculated efficiencies and peak-to-total ratio are shown in Table I for the various configurations.

Table I. Total photopeak efficiency and peak-to-total ratio calculated for EXOGAM. In configuration A, with partial Compton suppression, the 16 detectors are at 11.4 cm from the target point. In configuration B, with full suppression, the distance is 14.7 cm. The cube configuration consists in 4 Clovers with full suppression at 6.8 cm from the target. The measured value for the peak-to-total ratio in configuration B is 53%, about 10% less than the calculated values. This is most probably due to the approximate geometry used in the calculations.

	Phot. efficiency (%)		Peak-to-total (%)	
	662 keV	1.3 MeV	662 keV	1.3 MeV
Conf. A	28	20	57	47
Conf. B	17	12	72	60
Gamma-Cube	15	10	72	60

§3. Gamma-ray spectroscopy with radioactive beams from SPIRAL

3.1. Study of very deformed ground-state in neutron-deficient light rare-earth nuclei populated using ^{76}Kr beam and inverse kinematics

The first experiment I would like to describe was aiming at looking the very deformed ground-state in the light rare earth nuclei around ^{130}Sm . Hartree-Fock-Bogolyubov calculations using the D1S Gogny effective nucleon-nucleon interaction have been performed and indicate that these nuclei should have a *ground-state* deformation of $\beta \sim 0.40$ equivalent to the deformation measured for superdeformed bands in the Ce region. There are many open questions in this area. The evolution of the deformation when approaching the proton drip line is one of them. This is directly connected to the precise location of the neutron mid shell gap at $N = 64$. An interesting point related to very deformed nuclei, is the fact that the $\pi g_{9/2}$ orbital is very close to the Fermi surface. This level is known to have a dominant role in the occurrence of superdeformation for $A \sim 130$ nuclei. The questions are then: what is the wave function content of the active orbitals in the far off stability elements populated in this reaction? what is the influence of the $\pi g_{9/2}$ level on the nuclear shape close to the proton drip line?

Another fundamental interest in $N \sim Z$ nuclei, is the study of pairing correlations. Because N and Z are about equal, the active orbitals (orbitals occupied by valence particles) are the same and their overlap maximized. This leads to a large enhancement in the np correlations. For 'usual' pairing, nn and pp pairs are anti-aligned and occupy time reversed orbits, giving an isospin $T = 1$. For $N \sim Z$, np pairing is large. In that case, both $(T = 0, l = 0)$ and $(T = 0, l \neq 0)$ are possible. What are the effects of these correlated pairs on the wave functions? More precisely, Coriolis affect differently these kind of nucleon pairs. The signature of such a behaviour, could be a delayed alignment at "high" spin (some evidence have been

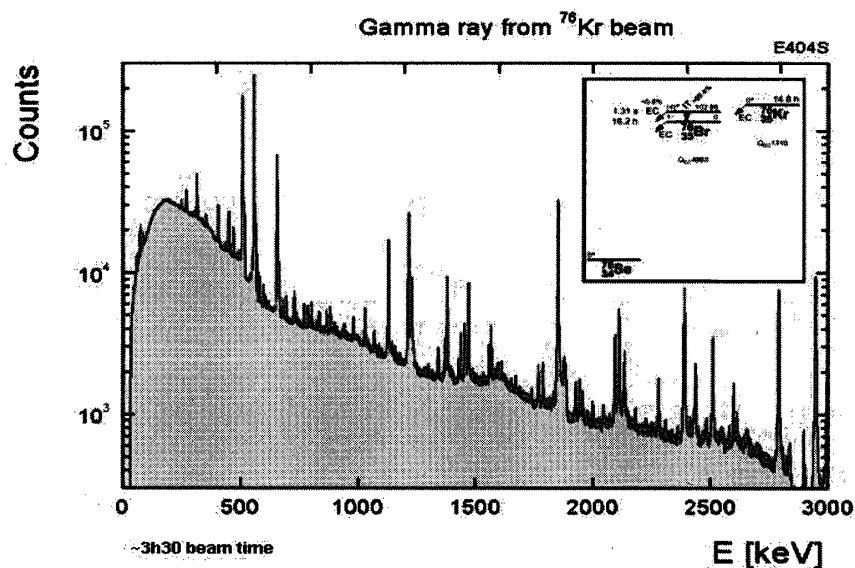


Fig. 2. Online raw spectrum obtained with after 3 h 30 min of ^{76}Kr beam time.

reported in Kr, Sr and Ru nuclei^(4)–9)) or a low spin signature inversion. These are some of the motivations for this run.

To produce these isotopes, we have used a ^{76}Kr beam with an intensity of $\sim 2 - 8 \times 10^5$ pps on a 1 mg/cm^2 ^{58}Ni target at 350 MeV. Six EXOGAM Clovers and 2 smaller ones were in the setup for this experiment which gave a photopeak efficiency of 11% at 344 keV. The DIAMANT charged particle detector was used together with the Debrecen chessboard (both consisting in CsI detectors: 24 cells for the chessboard and 2 rings of 16 cells for DIAMANT) to perform a better channel selection. The α and proton detection efficiency for this setup was approximately 70%. In this reaction, more than 10 channels were opened with a cross section larger than 10 mb: the calculated values are: $\sigma(^{130}\text{Nd}, ^{127}\text{Pr}) \sim 110$ mbarn; $\sigma(^{131}\text{Pm}, ^{128}\text{Nd}) \sim 35$ mbarn; $\sigma(^{130}\text{Pm}) \sim 25$ mbarn; $\sigma(^{131}\text{Sm}) \sim 2$ mbarn; $\sigma(^{130}\text{Sm}) < 1$ mbarn. An online gamma-ray spectrum corresponding to about 4 hours of beam time is shown in Fig. 2.

^{76}Kr has a $T_{1/2} = 14.8\text{h}$ which builds up into the target as well as in materials which is hit by the scattered beam. Without any particle selection it is not possible to observe any γ -ray from fusion events. The particle tagging allows us to clearly identify the $4p$, $3p$, $\alpha 2p$ and $\alpha 3p$ channels leading respectively to ^{130}Nd , ^{131}Pm , ^{128}Nd and ^{127}Pr (see Fig. 3) which are the most neutron-deficient known nuclei.

These spectra show that we have been able to observe the yrast band up to spin 18^+ in ^{130}Nd for example. This experiment, experienced several problems related to electronics, thunderstorm, noisy DIAMANT cell, etc. and will be rescheduled very soon. Nevertheless we have shown that the coupling of these two complex detectors is now operational and very efficient in selecting output channels. It was already

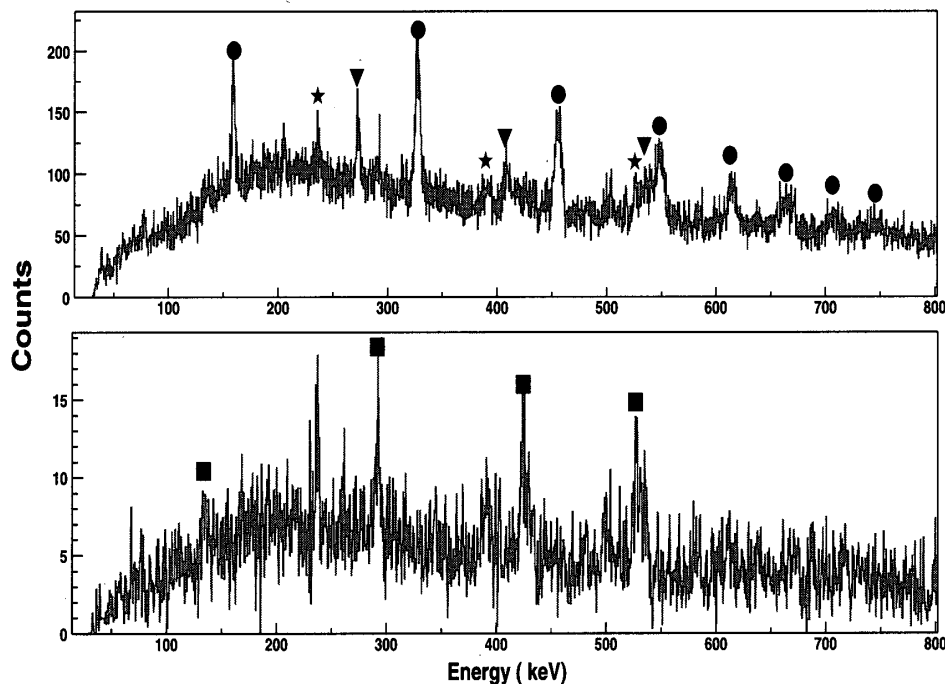


Fig. 3. γ -ray spectra obtained after demanding at least one proton (top) and at least one alpha (bottom) in DIAMANT. The symbols indicate γ -rays belonging to ^{130}Nd (circles), ^{131}Pm (triangles), ^{128}Nd (squares) and ^{127}Pr (stars).¹⁰⁾

known with stable beams induced fusion reaction that particle identification was really efficient and required when looking for neutron-deficient nuclei. For radioactive beam this is even more critical and we observe that all the radioactivity γ -ray lines have disappeared in the α or proton gated spectra. This was the first evidence of how the trigger conditions have to be carefully chosen in this kind of experiment.

3.2. Entrance channel effect on fusion cross-section using $^{6,8}\text{He}$ beams

The second experiment I want to focus on was aiming at investigating the entrance channel effects in the fusion process around the Coulomb barrier.^{11),12)} More precisely the idea was to look at the effect of the loosely bound neutrons in $^{6,8}\text{He}$ on the fusion with different isotopes to reach the same compound nucleus. The best target-projectile couples we have found was $^6\text{He} + ^{190}\text{Os}$ and $^8\text{He} + ^{188}\text{He}$ giving $^{196}\text{Pt}^*$. As a reference, we have run the $\alpha + ^{192}\text{Os}$ in Mumbai (India) using the TIFR-BARC pelletron tandem accelerator at various bombarding energies. The cross-sections obtained for this latter run is shown in Fig. 4. The backing for the Osmium targets was $^{63,65}\text{Cu}$ and this gave also very interesting results as will be shown later.

The specific difficulties of these type of measurements with SPIRAL beams are two fold: 1) measuring an excitation function with a cyclotron and 2) precise determination of the absolute cross-section and in particular with low intensity radioactive beams. This has been done using several tools to be able to cross-check the informations: highly sensitive Faraday cup, plastic detectors and annular segmented Si strip detector. For this run the EXOGAM implementation consisted in 5 EXOGAM

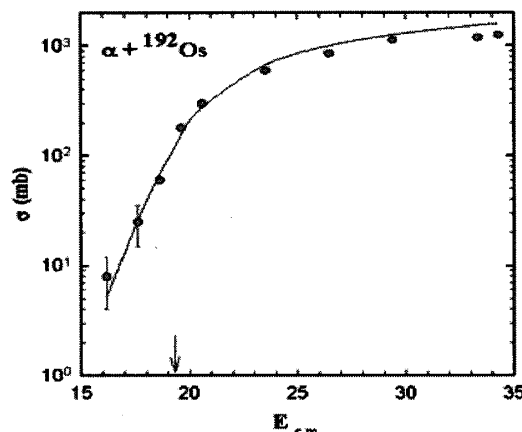


Fig. 4. Fusion cross-section for the ${}^4\text{He} + {}^{192}\text{Os}$ measured at the BARC-TIFR pelletron at Mumbai. The arrow indicates the position of the (1 dimensional) Coulomb barrier.

Clovers with their anti-Compton shield and 3 smaller Clovers. Knowing the array efficiency the beam intensity for ${}^8\text{He}$ has been measured to be 8×10^4 with a primary beam power of 1.2 KW at 27 MeV measured using the β -decay of ${}^8\text{He}$ on a thick Al target

Sub-barrier fusion is possible because of quantum mechanics. It is well known that the one dimensional (1D) barrier penetration model is far too simplistic and that the intrinsic structure of the colliding nuclei must be considered when one hopes to reproduce experimental data. It is also essential to take into account other channels like inelastic or transfer which are open at the same time. Because of its very special structure, it is interesting to use a halo nucleus as collision partner at energies close to the Coulomb barrier.

Expectations from various models are really diverging: some predict an enhancement of sub-barrier fusion cross-section while others give rise to flux reduction.¹³⁾⁻¹⁷⁾ Related to that is the effect of the coupling to break up channel. This was part of the motivations for this experiment. The idea was to measure absolute cross section via the γ -decay of the residues produced in fusion. The total fusion cross-sections being deduced from the summed partial cross-sections measured for each evaporation residue. The elastic channel was monitored by the annular silicon strip detector positioned at forward angles. The total intensity has been measured by a very sensitive Faraday cup (${}^6\text{He}$) and a plastic detector (${}^8\text{He}$). Typical spectra for the He+Cu (target backing) reaction are shown in Fig. 5.

The RF gated singles γ -ray spectra obtained with a radioactive beam are very clean. Gamma-rays from Cu isotopes also appear very clearly in coincidence with a charged particle in the Si detector. This corresponds to neutron transfer or incomplete fusion to the target. Statistical model calculations have been made with CASCADE which reproduce very nicely all the evaporation channels in the ${}^4\text{He}$ and ${}^6\text{He} + {}^{65}\text{Cu}$ except a single one: ${}^{66}\text{Cu}$ in ${}^6\text{He} + {}^{65}\text{Cu}$. CASCADE underestimate the cross section for this particular channel by more than one order of magnitude, pointing to evidence for a mechanism without compound nucleus formation. Similar calculations have been made for ${}^6\text{He} + {}^{63}\text{Cu}$, and again, the same channel is com-

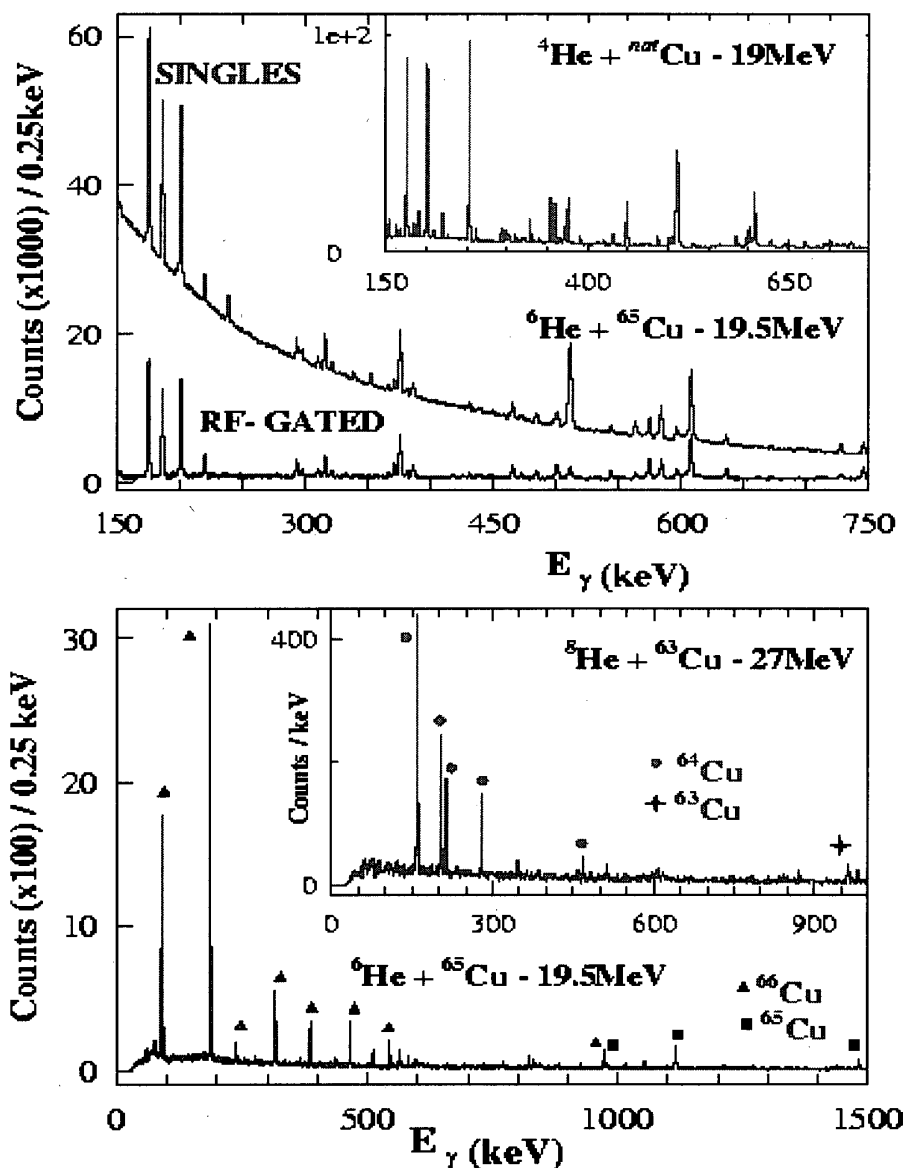


Fig. 5. Upper figure: Singles and RF gated γ -ray spectra for ${}^4\text{He} + {}^{\text{nat}}\text{Cu}$ and ${}^6\text{He} + {}^{65}\text{Cu}$. The bobarding energies are indicated. Lower figure: γ -ray spectra from ${}^6\text{He} + {}^{65}\text{Cu}$ and ${}^8\text{He} + {}^{63}\text{Cu}$ in coincidence with a charged particle in the Si detector. The main peaks are labeled.

pletely off the predictions (in that case ${}^{64}\text{Cu}$). The charged particle- γ coincidence spectra in the Silicon detector (the so-called 'Q-value' spectra) have been analyzed. A huge single peak is observed around $E \sim 16$ MeV for the ${}^6\text{He} + {}^{65}\text{Cu}$ run. This peak corresponds to $Q_{\text{opt}} \sim 0$, expected in the case of a neutron *transfer* mechanism. This is supported by the measured ratio of the various evaporation residues: with $E^* \gg S_{1n}$ and $E^* \sim S_{2n}$, ${}^{67}\text{Cu}$ is *not* observed while ${}^{66}\text{Cu}$ is. This ensemble of evidences is interpreted¹²⁾ as a direct observation of neutron transfer followed by evaporation. Therefore, and for the first time, it is possible to distinguish between break-up and transfer.

From the single gamma-ray spectra, the fusion and transfer cross sections have

been determined. For the transfer this lead to $\sigma_{transfer} \sim 335$ mbarn at 19.5 MeV and 355 mbarn at 30 MeV (which is about 30% of the complete fusion cross section). The reaction cross section sections have been deduced from the elastic scattering data measured by the Silicon strip detector in 5° to 50° angular domain. Finally, the break-up contribution $\sigma_{break-up} = \sigma_{reaction} - (\sigma_{fusion} + \sigma_{transfer})$ has been determined and shown to be roughly 50% lower than transfer, which is really surprising.

§4. Conclusions

The EXOGAM array and the SPIRAL facility have run a series of experiments in the last months. During these runs several auxiliary devices have been coupled to EXOGAM. This has been shown to be absolutely vital to eliminate the background and to obtain sensible gamma-ray spectra. In the next coming years, the experimental programme will develop at GANIL and there is no doubt that many challenging experiments will be run and will give new results.

Acknowledgements

At the end of this paper, I want to thank the spokespersons of the experiments which I have briefly described as well as the people who worked on the data: N. Redon, P. Nolan, O. Stezowski, A. Navin, J. M. Casandjian and the numerous collaborators who took part in one way or another to the experiments. My thanks are also going to the local engineers and technicians of GANIL who worked really hard and delivered very good beams in sometime difficult conditions and also took care of EXOGAM, in particular to J. Ropert and G. Voltolini.

References

- 1) GANIL web site, <http://www.ganil.fr/spiral/>
- 2) GANIL web site, <http://www.ganil.fr/exogam/>
- 3) GANIL web site, <http://www.ganil.fr/vamos/>
- 4) N. Marginean et al., PRC63.
- 5) N. Marginean et al., PRC65.
- 6) N. Marginean et al., PRC67.
- 7) D. Alber et al., Z. Phys. A **332** (1989), 129.
- 8) G. de Angelis et al., Phys. Lett. B **415** (1997), 223.
- 9) S. M. Fisher et al., Phys. Rev. Lett. **87** (2001), 132501.
- 10) O. Stezowski, private communication.
- 11) V. Tripathi et al., Phys. Rev. Lett. **88** (2002), 172701, and references therein.
- 12) A. Navin et al., submitted.
- 13) N. Takigawa and H. Sagawa, Phys. Lett. B **265** (1991), 23.
- 14) M. Hussein et al., Phys. Rev. C **46** (1992), 377.
- 15) C. H. Dasso and A. Vitturi, Phys. Rev. C **50** (1994), R12.
- 16) K. Hagino et al., Phys. Rev. C **61** (2000), 037602.
- 17) T. Nakatsukasa, Prog. Theor. Phys. Suppl. No. 154 (2004), 85.